frontiers in Earth Science

ORIGINAL RESEARCH
published: 05 May 2021
doi: 10.3389/feart.2021.617586

Sensitivity of Iodine-Mediated Stratospheric Ozone Loss Chemistry to Future Chemistry-Climate Scenarios

J. Eric Klobas[1]*, *Janina Hansen*[1], *Debra K. Weisenstein*[1,2], *Robert P. Kennedy*[1] and *David M. Wilmouth*[1]

[1] Harvard John A. Paulson School of Engineering and Applied Sciences, Harvard University, Cambridge, MA, United States, [2] Retired, Strafford, VT, United States

As the chemical and physical state of the stratosphere evolves, so too will the rates of important ozone-destroying reactions. In this work, we evaluate the chemistry-climate sensitivity of reactions of stratospheric iodine, reporting the iodine alpha factor (the efficiency of ozone loss mediated by a single iodine atom relative to the ozone loss mediated by a single chlorine atom) and the iodine eta factor (the efficiency of ozone loss mediated by a single iodine atom relative to the ozone loss mediated by a single chlorine atom in a benchmark chemistry-climate state) as a function of future greenhouse gas emissions scenario. We find that iodine-mediated ozone loss is much less sensitive to future changes in the state of the stratosphere than chlorine- and bromine-mediated reactions. Additionally, we demonstrate that the inclusion of the heterogeneous reaction of ozone with aqueous iodide in stratospheric aerosol produces substantial enhancements in the iodine alpha and eta factors relative to evaluations that consider gas-phase iodine reactions only. We conclude that the share of halogen-induced ozone loss due to reactions of iodine will likely be greater in the future stratosphere than it is today.

Keywords: stratospheric ozone, climate change, alpha factor, eta factor, iodine

OPEN ACCESS

Edited by:
Laura Revell,
University of Canterbury, New Zealand

Reviewed by:
Alfonso Saiz-Lopez,
Consejo Superior de Investigaciones Científicas, Spain
Jean-Baptiste Renard,
UMR7328 Laboratoire de Physique et Chimie de l'environnement et de l'Espace, France

***Correspondence:**
J. Eric Klobas
klobas@huarp.harvard.edu

Specialty section:
This article was submitted to Atmospheric Science, a section of the journal Frontiers in Earth Science

Received: *15 October 2020*
Accepted: *29 March 2021*
Published: *05 May 2021*

Citation:
Klobas JE, Hansen J, Weisenstein DK, Kennedy RP and Wilmouth DM (2021) Sensitivity of Iodine-Mediated Stratospheric Ozone Loss Chemistry to Future Chemistry-Climate Scenarios. Front. Earth Sci. 9:617586. doi: 10.3389/feart.2021.617586

1. INTRODUCTION

Until recently, iodine was thought to partition negligibly to the stratosphere due to the exceptionally short tropospheric lifetimes of the natural iodocarbons (Wennberg et al., 1997; Pundt et al., 1998; Bösch et al., 2003; Butz et al., 2009). With an approximate upper limit of total inorganic iodine of 0.15 pptv from these past studies, iodine was considered to play a negligible role in stratospheric ozone chemistry (Carpenter et al., 2014). However, Saiz-Lopez et al. (2015) demonstrated, by rectifying model projections with observations of IO in the TTL, that heterogeneous processes may enhance the efficiency of iodine injection enough to significantly increase stratospheric inorganic iodine. Recently, Koenig et al. (2020) provided quantitative evidence that total inorganic iodine may exist in the stratosphere at mixing ratios of approximately 0.8 pptv and that reactions of iodine may account for as much as a third of halogen-induced chemical ozone loss in the lower stratosphere.

While the total atmospheric inventories of inorganic bromine and chlorine are declining (Engel et al., 2018b), there exists evidence that the total atmospheric inorganic iodine inventory may be

increasing as a consequence of human activity (Prados Roman et al., 2015; Cuevas et al., 2018; Legrand et al., 2018). Additionally, evolving trends in the frequency and depth of tropopause-penetrating convective outflow and boundary layer ventilation (Trapp et al., 2009; Diffenbaugh et al., 2013; Seeley and Romps, 2015) may increase stratospheric I_y to even higher concentrations than present.

It follows that the rate and extent of important iodine-mediated catalytic cycles governing the thickness of the ozone layer are likely to change in the future. It is expected that the stratospheric burden of inorganic halogens will decline to levels observed in the year 1980 prior to the year 2060 as a result of continued global compliance with the Montreal Protocol on Substances that Deplete the Ozone Layer (and subsequent amendments; Newman et al., 2007; Engel et al., 2018a). Changes in the concentration and halogen character (i.e., the prevailing ratio of chlorine to bromine) of the stratospheric inorganic halogen inventory, as are expected during the slow differential decay of the various anthropogenic halocarbons, have been demonstrated to significantly impact the relative rates of bromine-, iodine-, and chlorine-mediated ozone destruction (Solomon et al., 1994; Danilin et al., 1996; Chipperfield and Pyle, 1998; Newman et al., 2007; Sinnhuber et al., 2009; Klobas et al., 2020).

Inorganic iodine (and to a lesser extent, inorganic bromine) is much more effective at catalyzing ozone loss than inorganic chlorine in part because compounds of inorganic iodine feature larger collisional cross sections, weaker bonds, and more red-shifted absorbance cross sections than their chlorine analogs. The alpha factor, α_X (X=Br or I), expresses this amplified ozone-destroying efficiency of a bromine or iodine atom relative to a chlorine atom and is defined in Equation (1) as a function of calendar date, t, location in the atmosphere, ρ, and chemical-climate state (e.g., boundary conditions corresponding to a specific moment in a specific climate scenario), ξ.

$$\alpha_X(t,\rho,\xi) = \frac{\Delta O_3(t,\rho,\xi)/\Delta X(t,\rho,\xi)}{\Delta O_3(t,\rho,\xi)/\Delta Cl(t,\rho,\xi)} \quad (1)$$

The annual-extrapolar average columnar value of α_I (i.e., ρ is integrated across longitude, altitude, and extrapolar latitudes and t is integrated across the calendar year) was estimated to be between 150 and 300 in the chemistry-climate state relating to the year 2002 (Ko et al., 2002), when extrapolar equivalent effective stratospheric chlorine (EESC) was near its peak concentration (Engel et al., 2018b). Likewise, annual-extrapolar average columnar α_{Br} is estimated to currently lie between 60 and 75 (Sinnhuber et al., 2009; Engel et al., 2018b; Klobas et al., 2020), with some variation between models and chemistry-climate boundary conditions (Daniel et al., 2006).

While α_{Br} or α_I presents the relative efficiency of the ozone-depleting effects of bromine or iodine at any given chemistry-climate state, the ratio to chlorine within the definition obscures the overall efficiency of halogen-mediated ozone depletion across different chemistry-climate states. For example, it is possible that α_{Br} or α_I increases as a chemistry-climate state evolves, while the actual extent of halogen-mediated ozone destruction declines as a result of slowing chlorine-mediated chemistry. Recently, Klobas et al. (2020) suggested using benchmark chemistry-climate state normalization as a technique to deconvolute simultaneous changes in the various halogen-mediated ozone destruction rates. The resulting eta factor metric, η_X (X=Cl, Br, or I), defined in Equation (2), facilitates a comparison of the extent of halogen-mediated ozone destruction across chemistry-climate states because it expresses the ozone-destroying efficiency of a chlorine, bromine, or iodine atom in an arbitrary chemistry-climate state, ξ, at calendar date, t, and location, ρ, relative to the ozone-destroying efficiency of a chlorine atom in a defined benchmark chemistry-climate state, Ξ.

$$\eta_X(t,\rho,\xi,\Xi) = \frac{\Delta O_3(t,\rho,\xi)/\Delta X(t,\rho,\xi)}{\Delta O_3(t,\rho,\Xi)/\Delta Cl(t,\rho,\Xi)} \quad (2)$$

Using a benchmark chemistry-climate state corresponding to $\Xi = 1980$, Klobas et al. (2020) demonstrate that while annually-averaged extrapolar total column α_{Br} is likely to only slightly decline or stay constant throughout the twenty-first century, depending on the greenhouse gas emissions scenario imposed, the actual extent of ozone loss mediated by bromine and chlorine varies to a much greater extent. This effect was most apparent in the most extreme climate change scenario evaluated by Klobas et al. (2020), where α_{Br} hardly changed, increasing by 4% from its year 1980 value of 70–73 in the year 2100, while η_{Cl} and η_{Br} declined precipitously by 35 and 33% over the same time interval, respectively. To date, neither α_I nor η_I have been assessed for possible chemistry-climate conditions of the future.

In this work, we use a 2-D chemical-transport-aerosol model informed by JPL-2019 photochemistry and kinetics (Burkholder et al., 2019) to provide the first estimates of α_I and η_I as a function of potential atmospheric chemistry-climate futures. Additionally, we evaluate the sensitivity of α_I and η_I to the recently highlighted direct heterogeneous reaction of ozone with aqueous iodide (Koenig et al., 2020). Furthermore, we demonstrate that, while rates of chlorine- and bromine-mediated ozone destruction show a clear dependence on future climate state, rates of iodine-mediated ozone destruction are less susceptible to perturbations in the physicochemical environment of the stratosphere, indicating that processes with the potential to rapidly transport short-lived iodine species directly into the stratosphere will be increasingly important as Earth's atmosphere evolves.

2. MODEL AND EXPERIMENT

The AER-2D chemical transport-aerosol model (Weisenstein et al., 1997, 2007) was employed for all results discussed in this work with a resolution of 19 latitudes and 51 vertical levels spanning 0–61 km. The model was informed by 315 kinetic reactions and 109 photochemical reactions, harmonized to JPL-2019 recommendations (Burkholder et al., 2019). Stratospheric sulfate aerosol microphysics and chemistry was fully prognostic, accounting for nucleation, coagulation, condensation/evaporation, sedimentation, and heterogeneous chemical interactions in a sectional manner (40 size bins).

All simulations employed specified dynamics corresponding to the 1978–2004 climatological average (e.g., eddy fields and streamfunctions). For evaluations of the historical past, climatologies were obtained from Fleming et al. (1999). Greenhouse gas boundary conditions for evaluations of future atmospheres were informed by the Representative Concentration Pathways (RCP) scenarios (Meinshausen et al., 2011; Van Vuuren et al., 2011), and Table 4-6 of the 2018 WMO Scientific Assessment of Ozone Depletion (World Meteorological Organization, 2018) informed boundary conditions for future halocarbons. Future climatological fields were obtained from the CMIP5 RCP experiments of MIROC-CHEM-ESM (Watanabe et al., 2011). All scenarios included an additional 5 pptv bromine from very short-lived bromocarbon sources (Wales et al., 2018).

The iodine chemical scheme was comprised of 10 iodine-containing species with 24 kinetic and 10 photolytic reactions. Iodine reactions were confined to those reactions explicitly prescribed by JPL-2019 (Burkholder et al., 2019) [excepting the photolysis of I_2O_2 parameterized per Davis et al. (1996), which was necessary for closure of the iodine chemical family]. While other reactions of iodine not included in the JPL-2019 chemical scheme have been studied in the literature, they typically have larger uncertainties and have not been evaluated by the NASA data panel. For example, JPL-2019 omits photochemical reactions of the higher oxides of iodine (e.g., I_2O_3 and I_2O_4) which may play a significant role in the iodine-mediated processing of ozone (Saiz-Lopez et al., 2012, 2014; Lewis et al., 2020). Importantly, these species are believed to enhance the burden of I_y in the upper troposphere and lower stratosphere (Saiz-Lopez et al., 2012, 2014). We mitigated the omission of this mechanism and others impacting stratospheric I_y by tuning the surface mixing ratio of CH_3I, the sole very short-lived emission source of iodine in this chemical scheme. The mixing ratio selected, 1.4 pptv, harmonized our calculated values of stratospheric IO and I_y with recent literature values (Saiz-Lopez et al., 2015; Engel et al., 2018b; Koenig et al., 2020).

Sensitivity studies involving the heterogeneous reaction of O_3 with I^-_{aq} were parameterized using a similar formulation as Koenig et al. (2020). The reactive uptake coefficient, γ, was formulated according to Equation (3).

$$\gamma_{O_3+I^-(aq)} = \frac{4H_{O_3}RTl_r k_{II}\left[I^-\right] f\left(l_r, r\right)}{\omega_{O_3}} \quad (3)$$

Here, H_{O_3} is the Henry's law constant with Sechenov correction, R is the gas constant, T is the temperature, l_r is the reacto-diffusive length, r is the radius corresponding to the aerosol size bin, k_{II} is the second order rate coefficient of the reaction, fit from Magi et al. (1997), $f(l_r, r)$ is the diffuso-reactive correction factor (Hanson et al., 1994), ω_{O_3} is the thermal velocity of O_3, and aqueous iodide concentrations were determined using the constants for the Henry's Law solubility of HI and HOI obtained from Ordóñez et al. (2012). Diffusion coefficients employed for the calculation of the diffusion-limited rate parameter and the diffuso-reactive distance were estimated as a function of viscosity using the parameterization of Reid et al. (1987) as informed by the Le Bas method. Dushman chemistry was implemented using kinetic constants fit from the data of Furuichi et al. (1972).

Halogen perturbation experiments were prepared using the method of Daniel et al. (1999): stratospheric chlorine, bromine, and iodine were perturbed via the surface emission of controlled quantities of proxy halocarbons ($CFCl_3A$, $CFBr_3$, or CFI_3). These proxy halocarbon species were constructed such that each has identical chemical kinetics and photochemistry with $CFCl_3$. Surface mixing ratios (constant at all latitudes) were carefully controlled to produce ozone deficits of less than 1% relative to the control experiment and are enumerated in **Table 1**. All experiments of a certain chemical-climatological condition were initialized from identical spun-up boundary conditions. Evaluations were conducted over a period of 20 model years, which was a sufficient time period to reach photochemical steady-state of the halocarbon perturbation proxy. The final 12 months of each experiment were used for data analysis. All permutations of the bracketed parameters indicated in **Table 1** were evaluated at constant chemical-climatological boundary conditions (time-slice) corresponding to the last year of each decade indicated (e.g., 1980, 1990,..., 2100).

Bromine and iodine alpha factors were computed per Equation (1) as extrapolar (60°S–60°N) annual averages. Ozone changes as a result of the halogen perturbation were computed as the difference between the perturbation scenario and the control experiment. Because the halocarbon proxy molecules share identical decomposition photochemistry and kinetics, the inorganic halogen scaling is simply the ratio of the halocarbon proxy molecule surface mixing ratios. Similarly, extrapolar annual-averaged chlorine, bromine, and iodine eta factors were computed in the manner of Klobas et al. (2020), per Equation (2). For all results in this work, we confined our analysis to the stratosphere ($z \geq 16$ km for annually-averaged extrapolar data).

3. RESULTS AND DISCUSSION

3.1. Evaluation of α and η When Including Gas-Phase Reactions of Iodine Only

For experiments in which only gas-phase reactions of iodine were considered in the iodine chemical scheme, decadal values of annually-averaged extrapolar columnar α_{Br} and α_I were calculated using historical data for scenarios occurring between the years 1980–2010 and RCP projections for each decade between 2020 and 2100. These values are presented in **Table 2** for both the historical past and the future. A visualization of these results is presented in **Figure 1** for extrapolar, annual-averaged (**Figure 1a**) α_{Br} and (**Figure 1b**) α_I. Percent deviations of these metrics from their year 1980 values are charted in **Figures 1c,d** for α_{Br} and α_I, respectively.

Klobas et al. (2020) evaluated the temporal dependence of extrapolar annual-average columnar α_{Br} for the same range of future dates and RCP emissions scenarios. We employed the same model and methodology in this work as was used in that study, except for the photochemistry and kinetics, which were previously harmonized to JPL-2015 recommendations (Burkholder et al., 2015) and did not include a refined iodine

TABLE 1 | Experiment schedule[a].

Experiment prefix	Decades[b]	Climatology	$CFCl_3A$ (pptv)	$CFBr_3$ (pptv)	CFI_3 (pptv)
bkg	[1980–2010]	historical[c]	0	0	0
bkg	[2020–2100]	RCP[2.6,4.5,6.0,8.5][d]	0	0	0
Cl	[1980–2010]	historical[c]	260	0	0
Cl	[2020–2100]	RCP[2.6,4.5,6.0,8.5][d]	260	0	0
Br	[1980–2010]	historical[c]	0	2.6	0
Br	[2020–2100]	RCP[2.6,4.5,6.0,8.5][d]	0	2.6	0
I	[1980–2010]	historical[c]	0	0	0.26
I	[2020–2100]	RCP[2.6,4.5,6.0,8.5][d]	0	0	0.26

[a] *Bracketed parameters were evaluated according to all permutations.*
[b] *Constant year for each decade (e.g., time slice: 1980, 1990, 2000).*
[c] *Informed by Fleming et al. (1999).*
[d] *Informed by Meinshausen et al. (2011) and Watanabe et al. (2011).*

TABLE 2 | Values of extrapolar (60°S–60°N) α_{Br} and α_I for historical and future scenarios[a].

Year	Historical		Year	RCP 2.6		RCP 4.5		RCP 6.0		RCP 8.5	
	α_{Br}	α_I		α_{Br}	α_I	α_{Br}	α_I	α_{Br}	α_I	α_{Br}	α_I
1980	71	126	2020	74	134	74	137	73	137	73	139
1990	74	131	2030	74	133	74	138	72	132	71	141
2000	75	132	2040	72	131	73	139	71	133	71	144
2010	74	136	2050	71	129	72	139	70	136	71	152
			2060	69	126	71	139	69	138	72	162
			2070	69	125	70	136	69	140	72	170
			2080	67	122	69	136	68	142	73	176
			2090	66	121	67	135	67	146	73	182
			2100	66	121	67	138	66	147	73	185

[a] *α_{Br} and α_I calculated per Equation (1).*
Historical temperature fields obtained from Fleming et al. (1999).
Historical and future greenhouse gas emissions specified per Meinshausen et al. (2011).
Future temperature fields derived from Watanabe et al. (2011).

chemical scheme. As a consequence, the bromine results reported here are very close, but not identical, to the results reported in Klobas et al. (2020) where α_{Br} peaked around the year 2000 at a value of 76 with a general trend of declining α_{Br} as the century progresses in the cases of RCP 2.6, RCP 4.5, and RCP 6.0. This trend is depicted in **Figure 1a**. We attribute a portion of this downward trend to a declining Cl_y:Br_y character of the stratosphere as the inorganic halogen inventory approaches natural levels. Under the emissions assumptions of RCP 8.5, α_{Br} remains relatively unchanged throughout the century as significant increases in emissions of N_2O and CH_4 counteract the changes in inorganic halogens.

The sensitivity of α_I to changes in chemistry-climate, as presented in **Figure 1b**, is qualitatively different than the behavior observed for α_{Br}. Under the assumptions of RCP 2.6, α_I declines slightly from its 1980 value by the end of the century as was observed with α_{Br}; however, unlike the case with bromine, α_I remains relatively stable, increasing slightly under the chemistry-climate assumptions of RCP 4.5 and RCP 6.0. In the circumstance of RCP 8.5, α_I increases by more than 45% relative to its 1980 value. A comparison of **Figures 1c,d** conveys this substantial difference in behavior between α_{Br} and α_I and speaks to an increasing relative importance of iodine to ozone as the chemistry-climate of the stratosphere evolves.

We note that the present-day values of α_I obtained from our analysis are in close agreement with the low estimate of the range, α_I = 150–300, reported in the most recent assessment of columnar α_I (Ko et al., 2002). There, the authors used a semiempirical ozone depletion potential (ODP) methodology to characterize α_I, per Equation (4), in which μ_X is the gram molecular weight of compound X, τ_X is the atmospheric lifetime of compound X, $n_X^{h_Z}$ is the number of halogen atoms of identity Z (Z=Cl, Br, or I) in compound X, ζ^I is equivalent to α_I as expressed in Equation (1), and ζ_X^D relates to the contribution of the compound under investigation to the distribution of inorganic halogen.

$$\mathrm{ODP}_{s-e}^{\text{long-lived}}(\mathrm{X}) = \frac{\mu_{\text{CFC-11}}}{\mu_{\mathrm{X}}} \times \frac{\tau_{\mathrm{X}}}{\tau_{\text{CFC-11}}} \times \frac{n_{\mathrm{X}}^{h_Z}}{n_{\text{CFC-11}}^{h_{\mathrm{Cl}}}} \times \left(\zeta^{\mathrm{I}} \times \zeta_{\mathrm{X}}^{\mathrm{D}}\right) \tag{4}$$

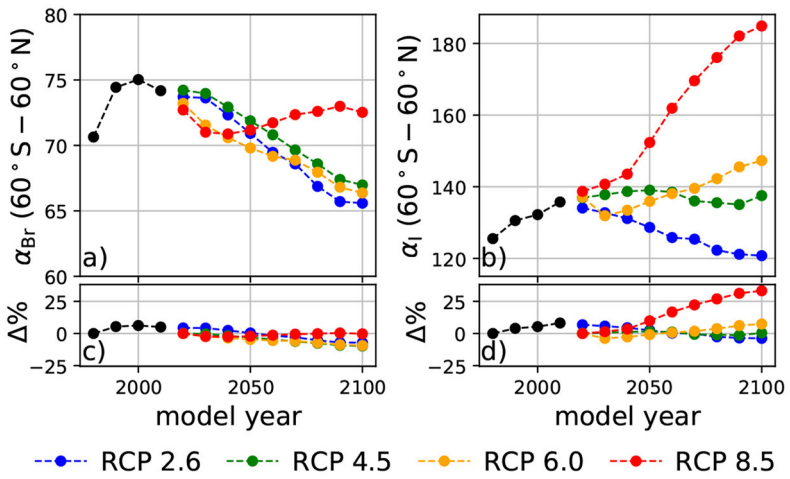

FIGURE 1 | Annual-average extrapolar (60°S–60°N) column α-factors as a function of RCP scenario in which only gas-phase reactions of iodine are considered. **(a)** α_{Br} and **(b)** α_I: black traces correspond to historical past and colored traces correspond to indicated RCP scenarios. **(c,d)** Percent deviation from 1980 value for α-factors presented in **(a,b)**, respectively.

Because our experiment utilizes CFC-11 proxies which are identical in all ways to CFC-11 except for the identity of the halogen released, we are able to probe for only ζ^I. This differs from the treatment described in Ko et al. (2002), as the technique used by the authors prevented the deconvolution of the product $\zeta^I \times \zeta_x^D$ due to their employment of CH_3I as the iodine source molecule. There, the authors state that it is possible that the value they derive of $\zeta^I \times \zeta_x^D = 300$ is due to $\zeta^I = 150$ and $\zeta_x^D = 2$ rather than ζ^I=300 and $\zeta_x^D = 1$. This supposition is reasonable, as the iodine source molecule in their determination, CH_3I, has a significantly shorter lifetime than CFC-11 in the lower stratosphere, and ζ_x^D should consequently be >1. A value of $\zeta^I = 150$ from Ko et al. (2002) would be in good agreement with our calculated values of α_I for the present day.

In order to examine the overall extent of halogen-mediated ozone loss processes in future chemistry-climate states, decadal, annually-averaged, extrapolar, columnar values of η_{Cl}, η_{Br}, and η_I were computed according to Equation (2). For all eta-factor calculations, the year 1980 was selected to be the chemistry-climate benchmark. These values are presented in **Table 3**. **Figure 2** presents columnar trends of η_{Cl} (**Figure 2a**), η_{Br} (**Figure 2b**), η_I (**Figure 2c**), and in **Figures 2d–f**, the percent deviation of each of these values from their 1980 value, respectively. As with α_{Br}, the results of η_{Cl} and η_{Br} are similar to the results of Klobas et al. (2020) as they were computed using the same methodology, boundary conditions, and a related model, but with updated JPL-2019 kinetics and a refined iodine chemical scheme.

Except in the case of RCP 2.6, η_{Cl} declines for all emissions scenarios as the century progresses, indicating a slowing of chlorine-mediated ozone chemistry as CH_4 and N_2O emissions increase. Under the end-of-century emissions assumptions of RCP 8.5, each additional stratospheric chlorine atom is only 62% as effective at destroying ozone as an additional stratospheric chlorine atom in an atmosphere representative of the chemistry-climate of the year 1980. Bromine chemistry is observed to slow under all future scenarios, as indicated in **Figure 2b**, in which η_{Br} shows a large dependence on the imposed chemistry-climate state. Under RCP 2.6 conditions, η_{Br} declines by 10%, ending the century at a value of 64 while under RCP 8.5 conditions, η_{Br} drops 37% from the 1980 value to 45 at the end of the century. Generally, η_{Br} follows the trend of η_{Cl} as rates of bromine- and chlorine-mediated ozone chemistry are sensitive to perturbations of CH_4, which directly reacts with chlorine and perturbs bromine chemistry indirectly, as well as to perturbations of NO_x from N_2O (Klobas et al., 2020).

Though η_I also declines in future scenarios, it does so less severely than either η_{Cl} or η_{Br}. End-of-century values of η_I range between 115 and 118 for all four RCP conditions, demonstrating considerably less variation across all chemistry-climate scenarios. This insensitivity of η_I is most evident in comparison of the percent deviation of the eta factors from their respective 1980 values in **Figures 2d–f**: while values of η_{Cl} and η_{Br} decline by more than 25% in some scenarios (and with considerable inter-scenario variation), η_I remains within 10% of the 1980 level in all chemistry-climate conditions evaluated.

The vertical dependence of η, presented in **Figure 3** for η_{Cl} (**Figure 3a**), η_{Br} (**Figure 3b**), and η_I (**Figure 3c**), further demonstrates the stability of iodine-mediated ozone chemistry to changing chemistry-climate conditions relative to bromine and chlorine. Though columnar η_{Cl} recovers nearly to its benchmark value by the end of the century when considering RCP 2.6, the vertical profile of η_{Cl} for the year 2100 shows significant differences from its behavior under the chemistry-climate conditions of 1980. The extent by which chlorine processes ozone is reduced by 34% at 18 km in the year 2100 while it increases by 32% at 45 km. There exists a clear acceleration of these temporal trends in η_{Cl} for RCP 8.5. Vertical profiles of

TABLE 3 | Values of extrapolar (60°S–60°N) η_{Cl}, η_{Br}, and η_I for historical and future scenarios[a].

Year	Historical			Year	RCP 2.6			RCP 4.5			RCP 6.0			RCP 8.5		
	η_{Cl}	η_{Br}	η_I		η_{Cl}	η_{Br}	η_I	η_{Cl}	η_{Br}	η_I	η_{Cl}	η_{Br}	η_I	η_{Cl}	η_{Br}	η_I
1980	1.0	71	126	2020	0.96	71	128	0.93	69	127	0.93	68	128	0.91	66	127
1990	0.99	73	129	2030	0.92	68	122	0.90	67	124	0.96	69	127	0.90	64	127
2000	0.96	72	127	2040	0.92	67	121	0.88	64	122	0.93	66	124	0.88	62	126
2010	0.93	69	126	2050	0.93	66	120	0.86	62	120	0.90	63	122	0.81	58	123
				2060	0.94	65	118	0.86	61	119	0.87	60	120	0.76	55	123
				2070	0.94	64	118	0.86	60	116	0.85	59	119	0.72	52	122
				2080	0.95	64	116	0.85	58	115	0.83	56	118	0.68	49	120
				2090	0.96	63	116	0.85	57	115	0.80	54	117	0.65	47	118
				2100	0.98	64	118	0.84	56	116	0.78	52	115	0.62	45	115

[a] *η_{Cl}, η_{Br}, and η_I calculated per Equation (2).*
Historical temperature fields obtained from Fleming et al. (1999).
Historical and future greenhouse gas emissions specified per Meinshausen et al. (2011).
Future temperature fields derived from Watanabe et al. (2011).

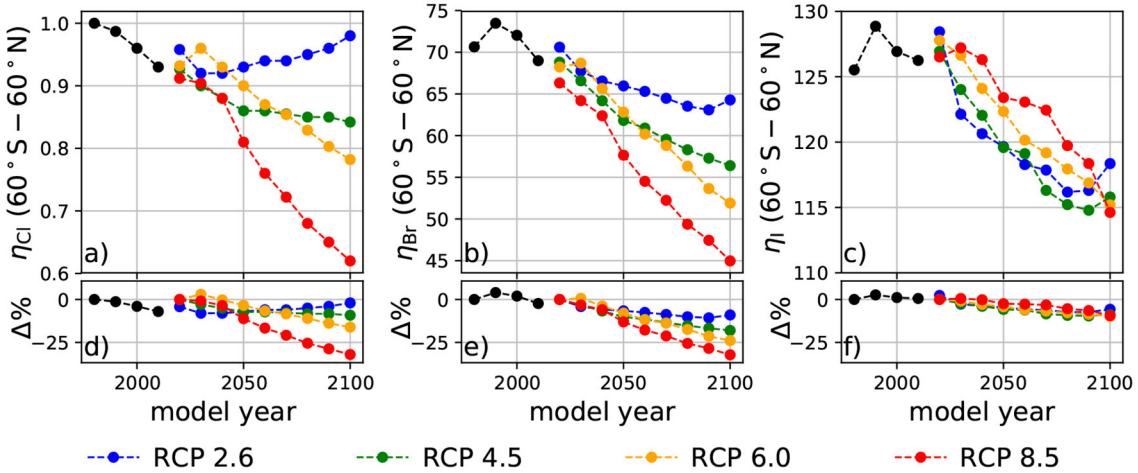

FIGURE 2 | Annual-average extrapolar (60°S–60°N) η-factors as a function of RCP scenario in which only gas-phase reactions of iodine are considered. **(a)** η_{Cl}, **(b)** η_{Br}, and **(c)** η_I: black traces correspond to historical past and colored traces correspond to indicated RCP scenarios. **(d–f)** Percent deviation from 1980 value for η-factors presented in **(a–c)**, respectively.

η_{Br} similarly demonstrate a sensitivity to the imposed chemistry-climate conditions with a considerable decrease at all altitudes below 30 km as time progresses in the RCP 8.5 experiment and a more moderate decrease over the same altitude range for evaluations of RCP 2.6. In contrast, there exists only slight variation of η_I between RCP scenarios and across time: an approximate 15% decrease in η_I relative to the 1980 benchmark chemistry-climate condition in the lower stratosphere between 16 and 25 km for the year 2100 for both RCP 2.6 and 8.5 chemistry-climate boundary conditions.

A sensitivity study was performed to determine the response of extrapolar column α_I and η_I to large perturbations in the emissions of N_2O, CH_4, and I_y. The results of this analysis are visualized in **Figure 4**. For each indicated perturbation condition in the vertical column, all other factors were constrained to their year 1980 values. The horizontal rows correspond to α_I (**Figures 4a–c**), η_{Cl} (**Figures 4d–f**), and η_I (**Figures 4g–i**). Klobas et al. (2020) present results for the investigation of the sensitivity of α_{Br}, η_{Cl}, and η_{Br} to similar perturbations; here, we expand their sensitivity analysis to also encompass iodine chemistry and use the updated JPL-2019 photochemistry and kinetics (Burkholder et al., 2019).

Following a nearly fourfold increase in N_2O (the range spanning the preindustrial mixing ratio of N_2O and twice the projected RCP 8.5 year 2100 concentration), we find in **Figure 4a** that α_I nearly doubles in magnitude. Meanwhile, a comparison of **Figures 4d,g** demonstrates that both η_{Cl} and η_I decline significantly as N_2O increases. Reactions of both chlorine and iodine are suppressed by the formation of the corresponding halogen nitrate as a consequence of increasing NO_2; however, the greater photolability of $IONO_2$

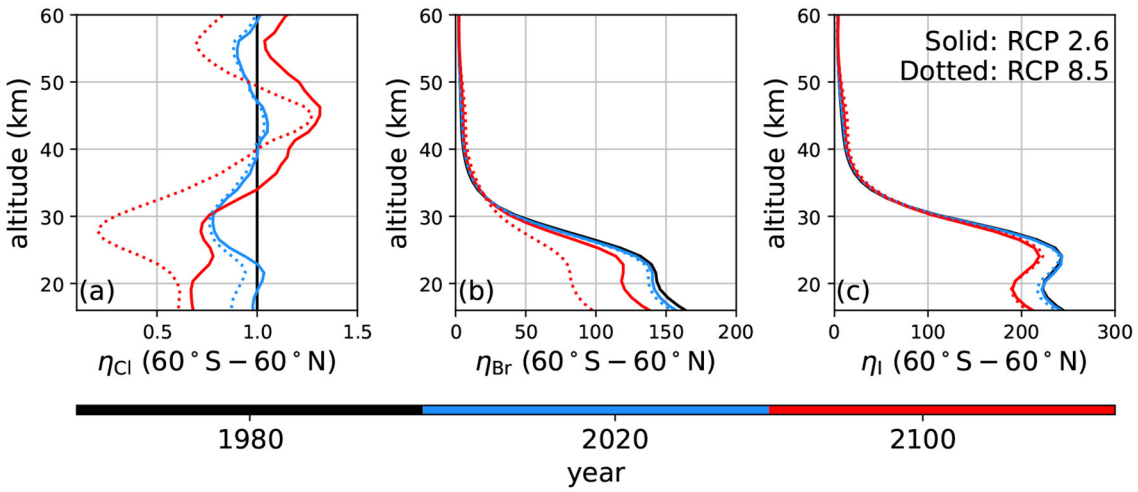

FIGURE 3 | Representative annual-average extrapolar (60°S–60°N) vertical profiles of **(a)** η_{Cl}, **(b)** η_{Br}, and **(c)** η_{I} in which only gas-phase reactions of iodine are considered. Solid lines: RCP 2.6 scenario. Dotted lines: RCP 8.5 scenario. Colors correspond to year of time-slice simulation as indicated by the colorbar.

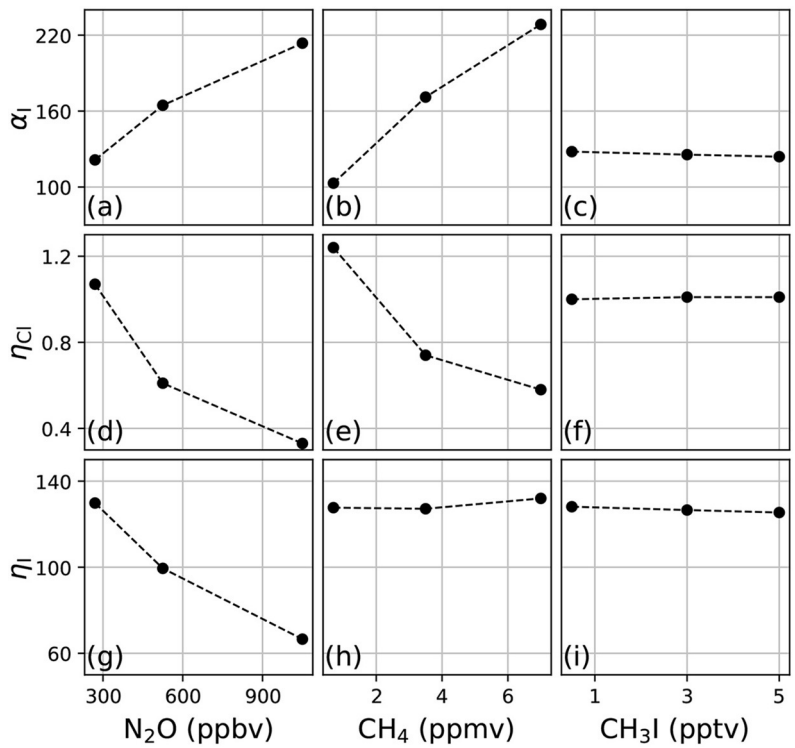

FIGURE 4 | Annual-average extrapolar (60°S–60°N) α- and η-factors as a function of the indicated perturbation. N_2O:**(a)** α_I, **(d)** η_{Cl}, **(g)** η_I. CH_4: **(b)** α_I, **(e)** η_{Cl}, **(h)** η_I. CH_3I: **(c)** α_I, **(f)** η_{Cl}, **(i)** η_I.

than $ClONO_2$ spurs the much larger magnitude reduction in η_{Cl} than the reduction in η_I. These differential changes drive the response of α_I.

The extent of ozone loss produced by stratospheric iodine chemistry is demonstrated to be relatively insensitive to large changes in CH_4 (ranging between preindustrial mixing ratios and twice the projected RCP 8.5 year 2100 concentration). In **Figure 4b**, the magnitude of α_I increases in tandem with ascending CH_4 mixing ratios. The extent of chlorine-driven ozone loss, η_{Cl}, is shown to decline significantly with increasing CH_4 in **Figure 4e**; however, the extent of iodine-driven ozone loss, η_I, shows very little change in **Figure 4h** with the same perturbation. While the direct reaction of the chlorine radical with CH_4 to form the hydrogen chloride reservoir occurs at

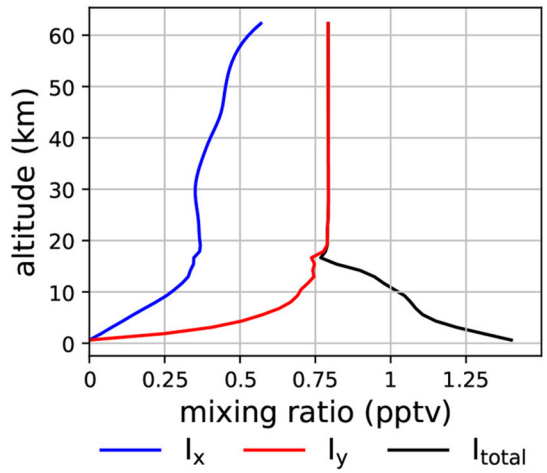

FIGURE 5 | Contemporary chemistry-climate scenario annual-average extrapolar (60°S–60°N) vertical profiles of active iodine (blue, I_x = I + IO), total inorganic iodine (red, $I_y = I_x + 2*I_2 + 2*I_2O_2 + INO + INO_2 + INO_3 + HOI + HI$), and total iodine (black, $I_{total} = I_y + CH_3I$) for experiments including heterogeneous iodine chemistry.

atmospherically relevant rates, the corresponding reaction of the iodine radical with CH_4 does not, which primarily explains the differing behaviors of η_{Cl} and η_I to increasing CH_4. Thus, the increasing magnitude of α_I with increasing CH_4 actually reflects the relative insensitivity of iodine to this perturbation that impacts chlorine and not an increase in the rates of iodine-mediated ozone chemistry.

Finally, an experiment was conducted to evaluate how changes in total stratospheric I_y might impact the metrics of interest. This was accomplished by titrating the surface mixing ratio of CH_3I approximately a factor of twenty, perturbing stratospheric I_y nearly proportionately. As CH_3I increases, very little variation (<3%) is observed for any of the metrics considered in **Figures 4c,f,i**, demonstrating that α_I and η_I are responsive to the differential changes in ozone produced by the perturbation gas and are not significantly impacted by uncertainties in the model-resolved levels of I_y.

3.2. Evaluation of α and η When Including Heterogeneous and Gas-Phase Reactions of Iodine

The rates and extent of iodine-mediated ozone catalysis are likely affected by the inclusion of the heterogeneous processing of ozone by iodide. Similarly, assumptions of chemistry-climate forcing are expected to perturb the rates and extent of this heterogeneous chemistry. In this section, we report α_I and η_I from model experiments in which heterogeneous processes of iodine are considered in addition to the gas-phase reactions of iodine employed in section 3.1.

When the direct reaction of ozone with aqueous iodide and subsequent Dushman chemistry is included in the iodine chemical scheme, total inorganic iodine, $I_y = I + 2*I_2 + IO + 2*I_2O_2 + INO + INO_2 + INO_3 + HOI + HI$, increases to approximately 0.8 pptv in the stratosphere from the gas-phase only experiment value of about 0.1 pptv. Similarly, active iodine, I_x = I + IO, produces a local maximum at 19 km of 0.37 pptv, increasing from a value of 0.03 pptv in the gas-phase only experiment. For the heterogeneous chemistry experiment, the vertical profiles of these families are illustrated in **Figure 5**, in which $I_{total} = I_y + CH_3I$ is also plotted. We note that our iodine chemical scheme does not reproduce known tropospheric trends in I_y and I_x because of our simplified iodine source chemistry; however, we demonstrate that stratospheric mixing ratios (above 16 km for extrapolar annual averages) and inorganic partitioning conform reasonably to expected literature values (Saiz-Lopez et al., 2015; Engel et al., 2018b; Koenig et al., 2020). At 16 km in the midlatitude lower stratosphere, where Koenig et al. (2020) report the only observation of IO in the stratosphere to date (0.06 ± 0.03 pptv), we obtain 0.11 pptv IO. This value exceeds the high boundary of 0.09 pptv IO reported by Koenig et al. (2020) by approximately 20%. At 24 km, where stratospheric sulfate aerosol surface area has decreased by 70% relative to levels at 16 km, our chemical scheme produces a maximal IO mixing ratio of 0.32 pptv. This value is lower than the result of approximately 0.45 pptv IO calculated in the ice-recycling scheme of Saiz-Lopez et al. (2015), but we note that their chemical scheme did not feature the gas-particulate partitioning of iodine on stratospheric sulfate aerosol which supresses $I_{y,gas}$ mixing ratios within the Junge layer. In the AER-2D model, the heterogeneous iodine chemical scheme results in a reduction in annually-averaged extrapolar ozone number density of 3% at 16 km relative to the gas-phase only experiment. This additional ozone loss quickly declines with altitude exhibiting a negligible difference in ozone number density between the two chemical schemes at 25 km.

Inclusion of heterogeneous iodine chemistry in the model approximately doubles total column α_I (reported in Section 3.1), as presented in **Figures 6a,c** and **Table 4**. This increased value of α_I is attributed almost entirely to the heterogeneous reaction and not the increased burden of I_y based on separate sensitivity studies in which CH_3I boundary conditions were perturbed substantially. As in the model realization without heterogeneous iodine chemistry, α_I within the RCP 8.5 scenario increases sharply as time progresses; however, the rate of increase in α_I in the heterogeneous iodine chemistry experiment is fourfold faster and more linear than in the case without heterogeneous iodine chemistry. We attribute this increase in α_I primarily to model prognostication of increased stratospheric aerosol density under RCP 8.5 conditions. The α_I values calculated in the RCP 2.6, RCP 4.5, and RCP 6.0 scenarios are qualitatively similar to their realizations in experiments without heterogeneous iodine chemistry, but scaled significantly larger.

Similarly, the inclusion of heterogeneous reactions in the chemical scheme does not create a substantial qualitative difference in the trajectories of η_I for the RCP 2.6, RCP 4.5, and RCP 6.0 experiments. As before, η_I is observed to remain fairly constant in time, as visualized in **Figures 6b,d** and enumerated in **Table 4**. As is the case with α_I, the η_I values calculated for the RCP 8.5 scenario demonstrate a divergence from the behavior of the other scenarios. In this case, η_I rapidly increases by 15% to a value of approximately 250, where it remains. In the other

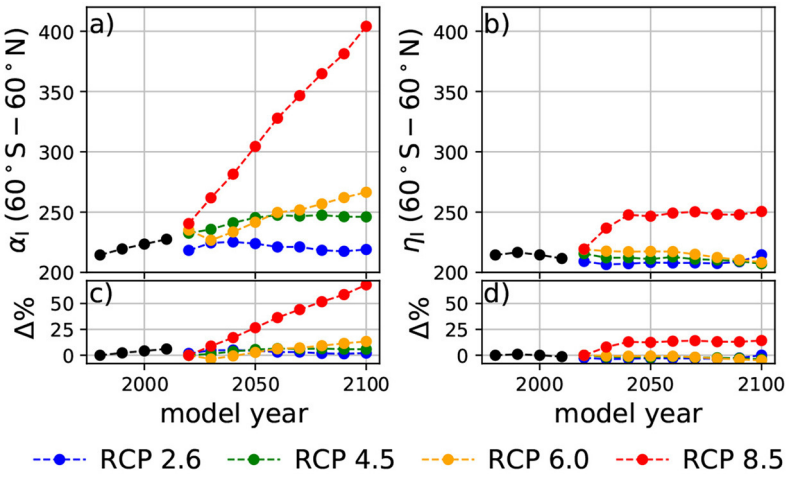

FIGURE 6 | Annual-average extrapolar (60°S–60°N) **(a)** α_I and **(b)** η_I as a function of RCP scenario when heterogeneous iodine chemistry is included: black traces correspond to historical past and colored traces correspond to indicated RCP scenarios. **(c,d)** percent deviation from 1980 value for α_I and η_I presented in **(a,b)**, respectively.

TABLE 4 | Values of extrapolar (60°S–60°N) α_I and η_I for historical and future scenarios with heterogeneous iodine chemistry[a].

Year	Historical		Year	RCP 2.6		RCP 4.5		RCP 6.0		RCP 8.5	
	α_I	η_I		α_I	η_I	α_I	η_I	α_I	η_I	α_I	η_I
1980	214	214	2020	218	209	233	216	235	219	241	219
1990	219	217	2030	224	207	236	212	227	218	262	237
2000	223	215	2040	225	208	241	212	234	217	281	248
2010	227	212	2050	224	208	245	211	242	217	304	247
			2060	221	208	247	213	250	217	328	249
			2070	221	208	247	211	252	215	347	250
			2080	218	207	247	210	257	212	365	248
			2090	218	209	246	209	262	210	381	248
			2100	219	215	246	207	266	208	404	251

[a] *α_I calculated per Equation (1). η_I calculated per Equation (2).*
Historical temperature fields obtained from Fleming et al. (1999).
Historical and future greenhouse gas emissions specified per Meinshausen et al. (2011).
Future temperature fields derived from Watanabe et al. (2011).

chemistry-climate scenarios, η_I is remarkably constant between different forcing conditions, remaining within the range of 207–219 for all scenario evaluations.

The trends in column α_I and η_I are driven primarily by the lower stratosphere. More than 75% of the ozone loss produced by the iodine perturbation occurs below 26 km, where the stratospheric aerosol layer primarily resides, while 60% of the ozone loss produced by the chlorine perturbation occurs above this altitude. When integrating over the annual-average extrapolar lower stratosphere (16–24 km) in a contemporary chemistry-climate scenario (RCP 2.6, year 2020), we recover a lower stratospheric column α_I of 456, which is approximately double the total column annual-average extrapolar α_I of 218 for the same chemistry-climate state.

Koenig et al. (2020) used a rates-based method to estimate a parameter similar to the alpha factor for the lower stratosphere, χ_Z/χ_{Cl}, where χ_Z is the instantaneous rate of ozone loss due to the members of halogen family Z (Z = Br or I). The method, defined in Equation (5), considers the instantaneous chemical loss rate due to odd oxygen, dO_x/dt, as a consequence of the reactions of the iodine or bromine family in ratio to the chemical loss rate of O_x due to the reactions of the chlorine family, where n_Z is the sum number density of the inorganic chemical species comprising halogen family Z.

$$\frac{\chi_Z}{\chi_{Cl}} = \frac{\frac{dO_{x,Z\ rxns}}{dt}/n_Z}{\frac{dO_{x,Cl\ rxns}}{dt}/n_{Cl}} \quad (5)$$

We note that this technique does not provide for the quantification of the impact of transport processes on local ozone, such that χ_I/χ_{Cl} is different from calculations of α_I; however, this method does facilitate the deconvolution of the local ozone-destroying efficiency of iodine into its component

parts. Koenig et al. (2020) estimate that χ_I/χ_{Cl} = 470 when considering both gas phase and heterogeneous chemistry in the lower stratosphere. Furthermore, the authors determine from estimates of iodine partitioning in the lower stratosphere that heterogeneous reactions of iodine provide $\chi_{I,\,het.}/\chi_{Cl}$ = 390, while gas phase reactions of iodine produce $\chi_{I,\,gas}/\chi_{Cl}$ = 980. Additionally, the authors determine χ_{Br}/χ_{Cl} = 69.8 for the same vertical integration.

We apply the rates-based method of Equation (5) and find an overall lower stratospheric column χ_I/χ_{Cl} of 424, with $\chi_{I,\,het.}/\chi_{Cl}$ = 361 and $\chi_{I,gas}/\chi_{Cl}$ = 678. Additionally, this method produces χ_{Br}/χ_{Cl}=72.6 with the same integration parameters. Thus, the overall values for our study and Koenig et al. (2020) agree within 10 and 4% for iodine and bromine, respectively. We note that our implementation of heterogeneous iodine chemistry slightly underestimates iodine particulate partitioning, with 79% of I_y in the particulate phase, relative to their estimates of 85% I_y partitioning. Overall, the consistency of the values we obtain using the rates-based method of Equation (5) with the results of Koenig et al. (2020) lends support to our calculated α and η factors.

4. CONCLUSIONS

In this work, a 2-D chemical-transport-aerosol model was employed to provide future estimates of α_I and η_I within the four RCP greenhouse gas emissions scenarios. These estimates demonstrate that for the gas-phase only experiments, in contrast to bromine, the relative ozone-destroying efficiency of iodine to chlorine (i.e., α_I) will largely remain the same, or substantially increase in the case of RCP 8.5, as the chemistry-climate state of the stratosphere evolves. We find that the temporal evolution of the ozone-destroying power of iodine (i.e., η_I) is observed to decline in all chemistry-climate scenarios evaluated; however, this effect is much less severe in the case of iodine than it is for most chemistry-climate evaluations of the other halogens. We conclude that the ozone chemistry of iodine is much less sensitive to changes in the chemical and physical state of the stratosphere than chlorine or bromine. In the future, the share of halogen-induced ozone loss due to reactions of iodine will likely be greater in the stratosphere than it is today.

When the direct reaction of ozone with aqueous iodine in aerosol is included in the model, we find a significant enhancement of α_I relative to the gas-phase-only iodine chemistry experiment. The local rates of iodine-mediated ozone processing obtained with our heterogeneous iodine chemistry scheme agree well with recent determinations obtained from analysis of *in situ* data. We find that the inclusion of heterogeneous iodine chemistry does not significantly alter the expected trend in η_I, except in the RCP 8.5 experiment in which η_I initially increases and then remains steady with time. Overall, the trends in the values of α_I and η_I are consistent between the gas-phase-only and heterogeneous iodine chemistry experiments; only the magnitude of the values changes significantly. Investigation of future iodine chemistry using more sophisticated parameterizations of iodine homogeneous and heterogeneous chemistry in a 3-D chemistry-climate-aerosol model would be valuable.

DATA AVAILABILITY STATEMENT

Publicly available datasets were analyzed in this study. The replication data may be obtained from the Harvard Dataverse: https://doi.org/10.7910/DVN/WBEYZJ.

AUTHOR CONTRIBUTIONS

JEK and DMW: concept. JEK, JH, RPK, and DKW: implementation. JEK: analysis. All authors contributed to discussion and preparation of the manuscript.

FUNDING

This research has been supported by the National Science Foundation, Division of Atmospheric and Geospace Sciences (Grant No. 1764171).

ACKNOWLEDGMENTS

We gratefully acknowledge funding support from the National Science Foundation. For our use of RCP temperature fields, we acknowledge the World Climate Research Programme's Working Group on Coupled Modeling, which is responsible for CMIP, and we thank the Japan Agency for Marine-Earth Science and Technology, Atmosphere and Ocean Research Institute (University of Tokyo), as well as the National Institute for Environmental Studies. JH thanks the Deutscher Akademischer Austauschdienst (DAAD) Research Internships in Science and Engineering (RISE) fellowship for financial support. RPK expresses gratitude to the Harvard College Office of Undergraduate Research and Fellowships for funding through the Program in Research in Science and Engineering (PRISE) fellowship. JEK thanks T. Sukhodolov and A. Karagodin-Doyennel for their consultation on the iodine chemical scheme.

REFERENCES

Bösch, H., Camy-Peyret, C., Chipperfield, M., Fitzenberger, R., Harder, H., Platt, U., et al. (2003). Upper limits of stratospheric IO and OIO inferred from center-to-limb-darkening-corrected balloon-borne solar occultation visible spectra: implications for total gaseous iodine and stratospheric ozone. *J. Geophys. Res.* 108:4455(D15). doi: 10.1029/2002JD003078

Burkholder, J. B., Sander, S. P., Abbatt, J. P. D., Barker, J. R., Cappa, C., Crounse, J. D., et al. (2019). *Chemical Kinetics and Photochemical Data for Use in Atmospheric Studies, Evaluation No. 19*. JPL Publication 19-5. Pasadena, CA: Jet Propulsion Laboratory.

Burkholder, J. B., Sander, S. P., Abbatt, J. P. D., Barker, J. R., Huie, R. E., Kolb, C. E., et al. (2015). *Chemical Kinetics and Photochemical Data for Use in Atmospheric*

Studies, Evaluation No. 18. JPL Publication 15-10. Pasadena, CA: Jet Propulsion Laboratory.

Butz, A., Bösch, H., Camy-Peyret, C., Chipperfield, M., Dorf, M., Kreycy, S., et al. (2009). Constraints on inorganic gaseous iodine in the tropical upper troposphere and stratosphere inferred from balloon-borne solar occultation observations. *Atmos. Chem. Phys*. 9, 7229–7242. doi: 10.5194/acp-9-7229-2009

Carpenter, L. J., Reimann, S., Burkholder, J. B., Clerbaux, C., Hall, B. D., Hassaini, R., et al. (2014). "Chapter 1: Update on Ozone-Depleting Substances (ODSs) and other gases of interest to the Montreal protocol," in *Scientific Assessment of Ozone Depletion: 2014, Global Ozone Research and Monitoring Project - Report No.55*, World Meteorological Organization, Geneva.

Chipperfield, M., and Pyle, J. (1998). Model sensitivity studies of arctic ozone depletion. *J. Geophys. Res*. 103, 28389–28403. doi: 10.1029/98JD01960

Cuevas, C. A., Maffezzoli, N., Corella, J. P., Spolaor, A., Vallelonga, P., Kjær, H. A., et al. (2018). Rapid increase in atmospheric iodine levels in the north Atlantic since the mid-20th century. *Nat. Commun*. 9, 1–6. doi: 10.1038/s41467-018-03756-1

Daniel, J. S., Solomon, S., Portmann, R., and Garcia, R. (1999). Stratospheric ozone destruction: the importance of bromine relative to chlorine. *J. Geophys. Res*. 104, 23871–23880. doi: 10.1029/1999JD900381

Daniel, J. S., Velders, G. J. M., Douglass, A. R., Forster, P. M. D., Hauglustaine, D. A., Isaksen, I. S. A., et al. (2006). "Chapter 8: Halocarbon scenarios, ozone depletion potentials, and global warming potentials," in *Scientific Assessment of Ozone Depletion: 2006, Global Ozone Research and Monitoring Project-Report No. 50*, World Meteorological Organization, Geneva.

Danilin, M. Y., Sze, N.-D., Ko, M. K., Rodriguez, J. M., and Prather, M. J. (1996). Bromine-chlorine coupling in the antarctic ozone hole. *Geophys. Res. Lett*. 23, 153–156. doi: 10.1029/95GL03783

Davis, D., Crawford, J., Liu, S., McKeen, S., Bandy, A., Thornton, D., et al. (1996). Potential impact of iodine on tropospheric levels of ozone and other critical oxidants. *J. Geophys. Res*. 101, 2135–2147. doi: 10.1029/95JD02727

Diffenbaugh, N. S., Scherer, M., and Trapp, R. J. (2013). Robust increases in severe thunderstorm environments in response to greenhouse forcing. *Proc. Natl. Acad. Sci. U.S.A*. 110, 16361–16366. doi: 10.1073/pnas.1307758110

Engel, A., Bönisch, H., Ostermöller, J., Chipperfield, M. P., Dhomse, S., and Jöckel, P. (2018a). A refined method for calculating equivalent effective stratospheric chlorine. *Atmos. Chem. Phys*. 18, 601–619. doi: 10.5194/acp-18-601-2018

Engel, A., Rigby, M., B, B. J., Fernandez, R. P., Froidevaux, L., D, H. B., Hossaini, R., Saito, T., et al. (2018b). "Chapter 1: Update on Ozone-Depleting Substances (ODS) and other gases of interest to the Montreal protocol," in *Scientific Assessment of Ozone Depletion: 2018, Global Ozone Research and Monitoring Project - Report No.58*, World Meteorological Organization, Geneva.

Fleming, E. L., Jackman, C. H., Stolarski, R. S., and Considine, D. B. (1999). Simulation of stratospheric tracers using an improved empirically based two-dimensional model transport formulation. *J. Geophys. Res*. 104, 23911–23934. doi: 10.1029/1999JD900332

Furuichi, R., Matsuzaki, I., Simic, R., and Liebhafsky, H. (1972). Rate of the dushman reaction at low iodide concentrations. experimental method and temperature coefficient. *Inorgan. Chem*. 11, 952–955. doi: 10.1021/ic50111a006

Hanson, D. R., Ravishankara, A., and Solomon, S. (1994). Heterogeneous reactions in sulfuric acid aerosols: a framework for model calculations. *J. Geophys. Res*. 99, 3615–3629. doi: 10.1029/93JD02932

Klobas, J. E., Weisenstein, D. K., J, S. R., and Wilmouth, D. M. (2020). Reformulating the bromine alpha factor and EESC: evolution of ozone destruction rates of bromine and chlorine in future climate scenarios. *Atmos. Chem. Phys*. 20, 9459–9471. doi: 10.5194/acp-20-9459-2020

Ko, M. K. W., Poulet, G., Blake, D. R., Boucher, O., Burkholder, J. B., Chin, M., et al. (2002). *Very Short-Lived Halogen and Sulfur Substances*. Geneva: World Meteorological Organization.

Koenig, T. K., Baidar, S., Campuzano-Jost, P., Cuevas, C. A., Dix, B., Fernandez, R. P., et al. (2020). Quantitative detection of iodine in the stratosphere. *Proc. Natl. Acad. Sci. U.S.A*. 117, 1860–1866. doi: 10.1073/pnas.1916828117

Legrand, M., McConnell, J. R., Preunkert, S., Arienzo, M., Chellman, N., Gleason, K., et al. (2018). Alpine ice evidence of a three-fold increase in atmospheric iodine deposition since 1950 in Europe due to increasing oceanic emissions. *Proc. Natl. Acad. Sci. U.S.A*. 115, 12136–12141. doi: 10.1073/pnas.1809867115

Lewis, T. R., Gómez Martín, J. C., Blitz, M. A., Cuevas, C. A., Plane, J. M. C., and Saiz-Lopez, A. (2020). Determination of the absorption cross sections of higher-order iodine oxides at 355 and 532 nm. *Atmos. Chem. Phys*. 20, 10865–10887. doi: 10.5194/acp-20-10865-2020

Magi, L., Schweitzer, F., Pallares, C., Cherif, S., Mirabel, P., and George, C. (1997). Investigation of the uptake rate of ozone and methyl hydroperoxide by water surfaces. *J. Phys. Chem. A* 101, 4943–4949. doi: 10.1021/jp970646m

Meinshausen, M., Smith, S. J., Calvin, K., Daniel, J. S., Kainuma, M., Lamarque, J.-F., et al. (2011). The RCP greenhouse gas concentrations and their extensions from 1765 to 2300. *Clim. Change* 109, 213–241. doi: 10.1007/s10584-011-0156-z

Newman, P. A., Daniel, J. S., Waugh, D. W., and Nash, E. R. (2007). A new formulation of equivalent effective stratospheric chlorine (EESC). *Atmos. Chem. Phys*. 7, 4537–4552. doi: 10.5194/acp-7-4537-2007

Ordó nez, C., Lamarque, J.-F., Tilmes, S., Kinnison, D. E., Atlas, E. L., Blake, D. R., et al. (2012). Bromine and iodine chemistry in a global chemistry-climate model: description and evaluation of very short-lived oceanic sources. *Atmos. Chem. Phys*. 12, 1423–1447. doi: 10.5194/acp-12-1423-2012

Prados Roman, C., Cuevas, C. A., Fernandez, R. P., Kinnison, D. E., Lamarque, J. F., and Saiz-lopez, A. (2015). A negative feedback between anthropogenic ozone pollution and enhanced ocean emissions of iodine. *Atmos. Chem. Phys*. 15, 2215–2224 doi: 10.5194/acpd-14-21917-2014

Pundt, I., Pommereau, J.-P., Phillips, C., and Lateltin, E. (1998). Upper limit of iodine oxide in the lower stratosphere. *J. Atmos. Chem*. 30, 173–185. doi: 10.1023/A:1006071612477

Reid, R., Prausnitz, J., and Poling, B. (1987). *The Properties of Gases and Liquids, 4th Edn*. New York, NY: McGraw-Hill.

Saiz-Lopez, A., Baidar, S., Cuevas, C. A., Koenig, T., Fernandez, R. P., Dix, B., et al. (2015). Injection of iodine to the stratosphere. *Geophys. Res. Lett*. 42, 6852–6859. doi: 10.1002/2015GL064796

Saiz-Lopez, A., Fernandez, R. P., Ordó nez, C., Kinnison, D. E., Gómez Martín, J. C., Lamarque, J.-F., et al. (2014). Iodine chemistry in the troposphere and its effect on ozone. *Atmos. Chem. Phys*. 14, 13119–13143. doi: 10.5194/acp-14-13119-2014

Saiz-Lopez, A., Plane, J. M. C., Baker, A. R., Carpenter, L. J., von Glasow, R., Gómez Martín, J. C., et al. (2012). Atmospheric chemistry of iodine. *Chem. Rev*. 112, 1773–1804. doi: 10.1021/cr200029u

Seeley, J. T., and Romps, D. M. (2015). The effect of global warming on severe thunderstorms in the united states. *J. Clim*. 28, 2443–2458. doi: 10.1175/JCLI-D-14-00382.1

Sinnhuber, B.-M., Sheode, N., Sinnhuber, M., Chipperfield, M., and Feng, W. (2009). The contribution of anthropogenic bromine emissions to past stratospheric ozone trends: a modelling study. *Atmos. Chem. Phys*. 9, 2863–2871. doi: 10.5194/acp-9-2863-2009

Solomon, S., Garcia, R. R., and Ravishankara, A. (1994). On the role of iodine in ozone depletion. *J. Geophys. Res*. 99, 20491–20499. doi: 10.1029/94JD02028

Trapp, R. J., Diffenbaugh, N. S., and Gluhovsky, A. (2009). Transient response of severe thunderstorm forcing to elevated greenhouse gas concentrations. *Geophys. Res. Lett*. 36:L01703. doi: 10.1029/2008GL036203

Van Vuuren, D. P., Edmonds, J., Kainuma, M., Riahi, K., Thomson, A., Hibbard, K., et al. (2011). The representative concentration pathways: an overview. *Clim. Change* 109, 5–31. doi: 10.1007/s10584-011-0148-z

Wales, P. A., Salawitch, R. J., Nicely, J. M., Anderson, D. C., Canty, T. P., Baidar, S., et al. (2018). Stratospheric injection of brominated very short-lived substances: aircraft observations in the western pacific and representation in global models. *J. Geophys. Res*. 123, 5690–5719. doi: 10.1029/2017JD027978

Watanabe, S., Hajima, T., Sudo, K., Nagashima, T., Takemura, T., Okajima, H., et al. (2011). Miroc-esm 2010: Model description and basic results of CMIP5-20c3m experiments. *Geosci. Model Dev*. 4:845. doi: 10.5194/gmd-4-845-2011

Weisenstein, D., Penner, J., Herzog, M., and Liu, X. (2007). Global 2-d intercomparison of sectional and modal aerosol modules. *Atmos. Chem. Phys*. 7, 2339–2355. doi: 10.5194/acp-7-2339-2007

Weisenstein, D. K., Yue, G. K., Ko, M. K., Sze, N.-D., Rodriguez, J. M., and Scott, C. J. (1997). A two-dimensional model of sulfur species and aerosols. *J. Geophys. Res.* 102, 13019–13035. doi: 10.1029/97JD00901

Wennberg, P., Brault, J., Hanisco, T., Salawitch, R., and Mount, G. H. (1997). The atmospheric column abundance of IO: implications for stratospheric ozone. *J. Geophys. Res.* 102, 8887–8898. doi: 10.1029/96JD03712

World Meteorological Organization (2018). *Scientific Assessment of Ozone Depletion: 2018, World Meteorological Organization, Global Ozone Research and Monitoring Project - Report No. 58*. World Meteorological Organization, Geneva.

Conflict of Interest: The authors declare that the research was conducted in the absence of any commercial or financial relationships that could be construed as a potential conflict of interest.